Spectrally Efficient Jamming Mitigation Based on Code-Controlled Frequency Hopping

Huahui Wang, Lei Zhang, Tongtong Li, and Jitendra Tugnait

***Abstract*—This paper considers spectrally efficient anti-jamming system design based on code-controlled frequency hopping. Unlike conventional frequency hopping systems where hopping patterns are determined by preselected pseudo-random sequences, in the proposed scheme, part of source information is passed through a block encoder, and used to determine the selected frequency bands for signal transmission. By exploiting the redundancy provided by the block coding, the receiver can retrieve the hopping pattern without a priori knowledge. Through an integrated decoding-and-encoding process, the receiver can also perform partial jamming detection. It is observed that due to the combination of dynamic frequency hopping and coding diversities, the proposed system can effectively mitigate random jamming interference while maintaining high spectral efficiency.**

***Index Terms*—Anti-jamming, frequency hopping.**

I. Introduction

FREQUENCY hopping has been widely used to combat unauthorized interception and hostile jamming attacks [1]. In conventional FH systems, each user hops independently based on a pre-specified pseudo-noise (PN) sequence. However, the spectral efficiency of the conventional FH is very low, even with high-dimensional constellations [2]–[6]. This limits its applicability in applications where the spectrum is restricted. Moreover, the jamming resistance property provided by conventional FH is inadequate, as once the PN sequence is compromised, follower jamming can be launched by the attacker.

To overcome the limitations of conventional FH, a message-driven frequency hopping (MDFH) was proposed in [7], [8]. By introducing an additional dimension into the signal space, MDFH can increase the spectral efficiency significantly (by multiple times) and can successfully prevent follower jamming due to the randomness provided by the encrypted message signal. Nevertheless, the performance of MDFH is determined by accurate detection of active channels (i.e., channels chosen for transmission).

Motivated by the MDFH scheme in [7], [8], in this letter, we propose a code-controlled message-driven frequency hopping scheme. Unlike MDFH where the majority of source data are used for hopping control, here only a small portion of source information is used to determine hopping frequencies. The rest of source information is modulated on the selected carriers. The randomness of the source data results in dynamic hopping patterns which can effectively prevent follower jamming. By integrating coding technique into the hopping frequency selection process, the proposed scheme can detect the active channels more accurately due to the inserted redundancy. As a result, under same spectral efficiency, the proposed scheme can achieve better anti-jamming effect than the MDFH scheme. Furthermore, such a coding scheme enables the receiver to partially detect jammed bands. The combination of dynamic frequency hopping and coding diversities results in strong anti-jamming capabilities. Simulation results demonstrate that the proposed system can effectively mitigate random jamming interference while maintaining high spectral efficiency.

Manuscript received January 13, 2010; revised May 23, 2010 and September 19, 2010; accepted December 13, 2010. The associate editor coordinating the review of this letter and approving it for publication was S. Blostein.

H. Wang, L. Zhang, and T. Li are with the Department of Electrical and Computer Engineering, Michigan State University, East Lansing, Michigan 48824, USA (e-mail: {wanghuah, zhangle3, tongli}@msu.edu).

J. Tugnait is with the Department of Electrical and Computer Engineering, Auburn University, Auburn, Alabama 36849, USA (e-mail: tugnajk@eng.auburn.edu).

Digital Object Identifier 10.1109/TWC.2011.010411.100057

II. Transmitter Design of Code-Controlled FH

The transmitter structure of the proposed system is illustrated in Fig. 1. The input binary stream $\{a_i\}$ is passed through a rate-R encoder ENC_1 and an interleaver π, then is demultiplexed (DEMUX) into two branches. In the lower branch, a K-bit data vector $\mathbf{a} = [a_1, a_2, \cdots a_K]$ is fed into a rate K/N block encoder ENC_2, producing an N-bit codeword $\mathbf{b} = [b_1, b_2, \cdots b_N]$. The code generated from ENC_1 is called the *outer code* and the concatenated block code from ENC_2 is called the *inner code*. The inner code is chosen in such a way that the total number of 1's in the codeword, $L = \sum_{i=1}^{N} b_i$, is a fixed number for any K-bit input $\mathbf{a} = [a_1, a_2, \cdots a_K]$, as long as $\mathbf{a}$ is not an all-zero vector. Codes possessing such property are called "constant weight codes", and there are various approaches to constructing these codes. One popular way is to use the Hadamard codes [9]. When an (N, K) Hadamard code is employed, then $N = 2^{(K-1)}$ and $L = N/2$. This code has such a strong error-correction capability that it can correct up to $t = N/4 - 1$ errors.

Although it is a rare situation, yet if there is an all-zero input, the first element of the input vector $\mathbf{a}$ is toggled into "1". The introduced one-bit error will rely on the outer code to correct.

The upper branch of the transmitter employs an M-ary symbol mapper with each symbol containing $m = \log_2 M$ bits. The number of bits entering the upper branch is mL, such that a total number of L symbols are generated from the upper branch, denoted here as $\mathbf{d} = [d_1, d_2, \cdots, d_L]$. The symbol vector $\mathbf{d}$ is first fed to a serial-to-parallel (S/P) converter and then transmitted simultaneously through L selected subcarriers of an N-carrier system. These L active subcarriers are determined by the N-bit codeword $\mathbf{b} = [b_1, b_2, \cdots b_N]$ generated in the lower branch. Let $\{\omega_1, \omega_2, \cdots, \omega_N\}$ be all the carrier frequencies in the system. For $i = 1, \cdots, N$, if $b_i = 1$, the carrier centered at ω_i is selected for data modulation; otherwise, if $b_i = 0$, the carrier centered at ω_i becomes idle.

In other words, input binary stream $\{a_i\}$ is always divided into blocks of length $L_b = (mL + K)R$, which is set to be an

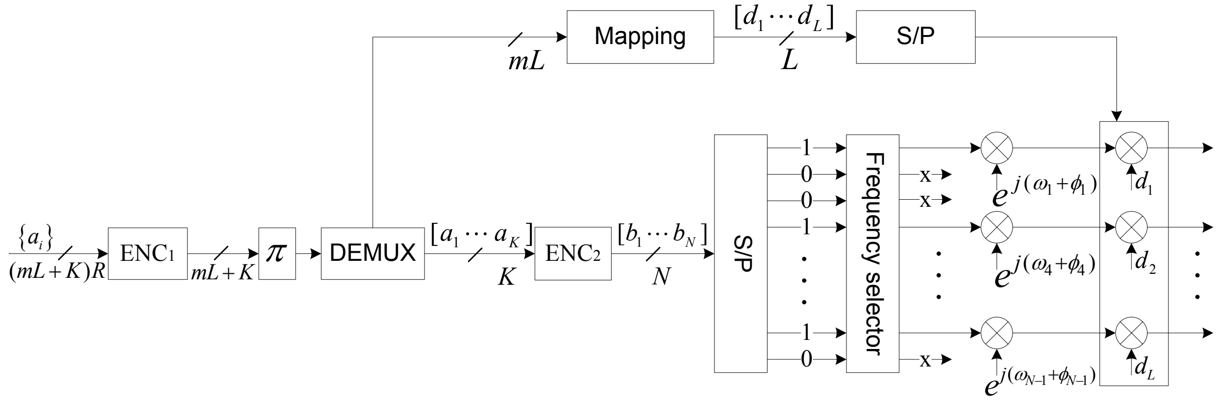

Fig. 1. Block diagram of transmitter structure.

integer. Assume the input bit period is T_b. During each block interval $T_s = (mL+K)RT_b$, the transmitted signal on the ith carrier, $s_i(t)$, can be expressed as

$$s_i(t) = s_i e^{j(\omega_i t+\phi_i)}, \tag{1}$$

where s_i is the signal symbol transmitted over carrier i and ϕ_i is a random phase uniformly distributed over $(0, 2\pi]$, which is generally caused in the modulation process and can be tracked at the receiver [10]. s_i can be represented as

$$s_i = \begin{cases} 0, & b_i = 0; \\ d_{\ell(i)}, & b_i = 1. \end{cases} \tag{2}$$

Here the subscript $\ell(i) = \sum_{k=1}^{i} b_k$ indicates the index of the upper branch symbol modulated on the ith carrier. By defining $d_0 = 0$, Eq. (2) can be simplified as

$$s_i = b_i d_{\ell(i)}. \tag{3}$$

Remark 1: *The proposed system can be directly extended to a multi-user system in different ways. For downlink transmission, different users' data can be multiplexed into one stream $\{a_i\}$ for transmission. For the uplink, multiple access can be achieved by combining the proposed scheme with TDMA or wideband FDMA.*

III. Receiver Design

We assume that the system is subjected to partial-band jamming, for which the total jamming power J watts is uniformly distributed over a fraction ρ of the system bandwidth W Hz. If the bandwidth of each carrier/channel is B Hz, the jamming power in one jammed channel is given by

$$\sigma_j^2 = (\frac{J}{\rho W})B \quad watts. \tag{4}$$

The received signal $r_i(t)$ for the ith channel can be written as

$$r_i(t) = s_i(t) + \theta_i j_i(t) + n_i(t), \tag{5}$$

where $n_i(t)$ and $j_i(t)$ represent system noise and jamming interference, respectively. They are assumed to be statistically independent zero-mean complex Gaussian processes [11], with $\frac{1}{2}E\{|n_i(t)|^2\} = \sigma_n^2$ and $\frac{1}{2}E\{|j_i(t)|^2\} = \sigma_j^2$. Define

$$\theta_i = \begin{cases} 1, & j_i(t) \text{ is present in } r_i(t), \\ 0, & j_i(t) \text{ is absent from } r_i(t). \end{cases} \tag{6}$$

Then θ_i is a binary random variable with $P\{\theta_i = 1\} = \rho$ and $P\{\theta_i = 0\} = 1 - \rho$.

A. Receiver Structure

The block diagram of the receiver is shown in Fig. 2.

The received signal at the ith channel is extracted as

$$\begin{aligned} r_i &= \frac{1}{T_s}\int_0^{T_s} r_i(t) e^{-j(\omega_i t+\phi_i)} dt \\ &= b_i d_{\ell(i)} + \theta_i j_i + n_i, \end{aligned} \tag{7}$$

where j_i and n_i are zero-mean Gaussian variables with $\frac{1}{2}E\{|j_i|^2\} = \sigma_j^2$ and $\frac{1}{2}E\{|n_i|^2\} = \sigma_n^2$.

The source information is embedded in the first term of (7), i.e., $b_i d_{\ell(i)}$. We first retrieve b_i to determine the pattern of carrier selection, and then recover $d_{\ell(i)}$ from the channel where $b_i = 1$. The estimate of $\mathbf{b} = [b_1, b_2, \cdots b_N]$, denoted as $\tilde{\mathbf{b}} = [\tilde{b}_1, \tilde{b}_2, \cdots \tilde{b}_N]$, is determined according to the following criterion:

$$\tilde{b}_i = \begin{cases} 1, & |r_i|^2 \geq \gamma; \\ 0, & |r_i|^2 < \gamma, \end{cases} \tag{8}$$

where γ is the detection threshold, whose optimum value can be determined by minimizing the error probability $p = P\{b_i \neq \tilde{b}_i\}$, as discussed in Section III-B.

The estimate $\tilde{\mathbf{b}} = [\tilde{b}_1, \tilde{b}_2, \cdots \tilde{b}_N]$ is a rough decision since errors can be easily introduced by jamming interference. To make the estimate more reliable, we propose a decoding-and-encoding process at the receiver, as shown in Fig. 2. The rough decisions in $\tilde{\mathbf{b}}$ are parallel to serial converted, and passed to the block decoder DEC_2 which corresponds to ENC_2 at the transmitter. If the Hadamard code is constructed from the Hamadard matrix $\mathbf{H}$ and its complementary $-\mathbf{H}$ with each -1 replaced by 0, the decoding can be performed as below: Transform $\tilde{\mathbf{b}}$ to a $1/-1$ vector $\mathbf{v}$ by changing all 0s to -1 and then compute $\mathbf{v}\mathbf{H}^T$. The entry with the maximum absolute value corresponds to the row taken as a codeword. The codeword came from $\mathbf{H}$ if it is positive; otherwise it came from $-\mathbf{H}$. The decoded information is then obtained by transforming the determined row index into binary bits.

The decoder outputs $\hat{\mathbf{a}} = [\hat{a}_1, \hat{a}_2, \cdots \hat{a}_K]$ are the recovered signal bits corresponding to $\mathbf{a}$. Following DEC_2, we employ an encoder same as ENC_2, which encodes $\hat{\mathbf{a}} = [\hat{a}_1, \hat{a}_2, \cdots \hat{a}_K]$ to produce $\hat{\mathbf{b}} = [\hat{b}_1, \hat{b}_2, \cdots \hat{b}_N]$. Compared with

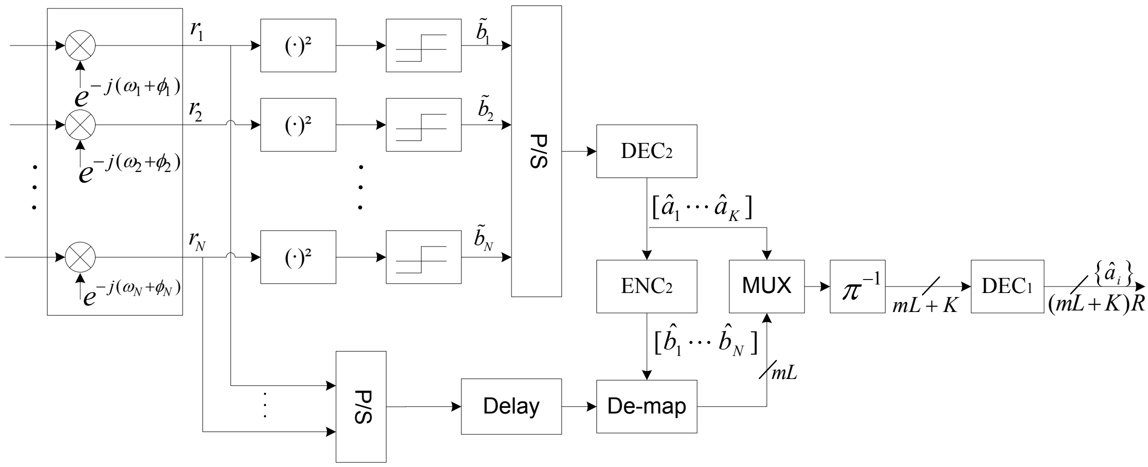

Fig. 2. Block diagram of receiver design.

$\tilde{\mathbf{b}}$, $\hat{\mathbf{b}}$ is a much more accurate version of $\mathbf{b}$, since errors in $\tilde{\mathbf{b}}$ could be corrected after decoder DEC_2.

Remark 2: *In a jamming-dominant system, errors in* $\tilde{\mathbf{b}}$ *mainly result from jamming interference. In such cases, calculating the set of indices* $\mathcal{J} = \{k \mid \tilde{b}_k = 1,\ \hat{b}_k = 0,\ 1 \le k \le N\}$ *will reveal the bands that are jammed. Hence the proposed scheme has the side effect of jamming detection. This capability is useful in applications such as cognitive radio networks, where spectrum sensing technologies should be employed to detect whether the spectrum is used ("jammed") or not.*

After obtaining $\hat{\mathbf{b}}$, the set of carriers $\mathcal{I}$ selected for transmission is given by $\mathcal{I} = \{k \mid \hat{b}_k = 1,\ 1 \le k \le N\}$. The received signal r_i on channel $\{i \in \mathcal{I}\}$ is then demodulated to retrieve the upper branch signals. The demodulator outputs, multiplexed with the estimated lower branch bits, are then fed to the deinterleaver π^{-1}, followed by decoder DEC_1, to obtain the recovered signal.

The jamming mitigation capability of the proposed system results from dynamic frequency hopping, as well as the time-frequency diversity introduced by the two channel encoders. The random frequency hopping makes it hard for the jammer to determine the hopping pattern, and hence prevents the follower jamming. Furthermore, the errors caused by the jamming can be partially or totally recovered by the channel coding, depending on the error correction capability of the codes as well as the level of jamming interference. The system performance under various jamming scenarios is illustrated in Section V.

B. Optimal Threshold Selection

The average error probability of b_i in the lower branch, denoted as $\bar{p}$, depends on jamming conditions. If the output of the block encoder ENC_2 always has an equal number of 1's and 0's, as in the Hadamard code, it then follows from Eqs. (6) and (8) that:

$$\begin{aligned}\bar{p} &= \sum_{b_i=0,1} P\{b_i \neq \hat{b}_i | b_i\} P\{b_i\} \\ &= \frac{1}{2} \sum_{b_i=0,1} \sum_{\theta_i=0,1} P\{b_i \neq \hat{b}_i | b_i, \theta_i\} P\{\theta_i\} \\ &= \frac{1}{2}[(1-\rho)p_1 + \rho p_2] + \frac{1}{2}[(1-\rho)p_3 + \rho p_4] \quad (9)\end{aligned}$$

where $\rho = P\{\theta_i = 1\}$ and $1 - \rho = P\{\theta_i = 0\}$, and the conditional probabilities $p_1, \cdots, p_4$ can be calculated as follows.

The probability of p_1 is given by

$$\begin{aligned}p_1 &= P\{|r_i|^2 < \gamma \big| b_i = 1, \theta_i = 0\} \\ &= P\{|d_{\ell(i)} + n_i|^2 < \gamma\} \\ &= 1 - Q_1\left(\frac{|d_{\ell(i)}|}{\sigma_n}, \frac{\sqrt{\gamma}}{\sigma_n}\right), \quad (10)\end{aligned}$$

where $|d_{\ell(i)}|$ is the square-root of the modulated signal power, and function $Q_1(a, b)$ is the Marcum's Q function defined as [9]

$$Q_1(a, b) = e^{-(a^2+b^2)/2} \sum_{k=0}^{\infty} \left(\frac{a}{b}\right)^k I_k(ab). \quad (11)$$

Here $I_k(x)$ is the kth order modified Bessel function of the first kind.

Similarly,

$$\begin{aligned}p_2 &= P\{|r_i|^2 < \gamma \big| b_i = 1, \theta_i = 1\} \\ &= 1 - Q_1\left(\frac{|d_{\ell(i)}|}{\sqrt{\sigma_n^2 + \sigma_j^2}}, \frac{\sqrt{\gamma}}{\sqrt{\sigma_n^2 + \sigma_j^2}}\right), \quad (12)\end{aligned}$$

and

$$\begin{aligned}p_3 &= P\{|r_i|^2 \ge \gamma \big| b_i = 0, \theta_i = 0\} \\ &= e^{-\gamma/\sigma_n^2}, \quad (13)\end{aligned}$$

$$\begin{aligned}p_4 &= P\{|r_i|^2 \ge \gamma \big| b_i = 0, \theta_i = 1\} \\ &= e^{-\gamma/(\sigma_n^2+\sigma_j^2)}. \quad (14)\end{aligned}$$

The optimal threshold γ_{opt} can be determined through

$$\gamma_{opt} = \arg\min_{\gamma} \bar{p}. \quad (15)$$

The closed-form solution of γ_{opt} is hard to find, but numerical results can be obtained through an exhaustive search. Fortunately, simulation results have shown that system performance is not very sensitive to γ. As will be shown in Section V, satisfying performance can still be achieved even if γ varies over a wide range. In practice, when a rough estimation of jamming interference and noise power is obtained, γ can be set to be slightly above the power level of the interference and the noise.

IV. Spectral Efficiency

To ensure orthogonality between the subcarriers, the frequency spacing between adjacent carriers is set to be $\Delta f = 1/T_s$. The total bandwidth W required for the system depends on whether adjacent carriers are overlapped or not. If the overall frequency band is divided into N nonoverlapping subchannels and signals are frequency-multiplexed, the total system bandwidth, denoted here as W_{FDM}, is given by $W_{FDM} = \frac{2N}{T_s} = \frac{2N}{(mL+K)RT_b}$. The corresponding spectral efficiency η_{FDM} is then given by

$$\eta_{FDM} = \frac{(mL+K)R}{2N} \quad \text{bits/s/Hz}. \tag{16}$$

Otherwise, if carriers are arranged in a way similar to that of Orthogonal Frequency Division Multiplexing (OFDM), the required bandwidth, W_{OFDM}, is given by $W_{OFDM} = \frac{N+1}{T_s} = \frac{N+1}{(mL+K)RT_b}$. The corresponding spectral efficiency η_{OFDM} is

$$\eta_{OFDM} = \frac{(mL+K)R}{N+1} \quad \text{bits/s/Hz}. \tag{17}$$

Therefore, by using OFDM modulation technique, we could almost double the spectral efficiency. However, as will be demonstrated in the simulation examples, there is always a tradeoff between the spectral efficiency and anti-jamming capability.

V. Simulation Results

Simulations are conducted to evaluate the system performance. For purpose of comparison, the signal power S for each incoming bit and the total injected jamming power J are fixed for all systems. The signal to jamming interference ratio is defined as $SJR = S/J$, and the signal to noise ratio is defined as $SNR = E_b/N_0$. The SNR of 8dB is used unless otherwise stated. Lower branch encoding employs the $(N, K) = (128, 8)$ Hadamard code. $L = N/2 = 64$. Symbol mapping uses the 8-PSK constellation. Convolutional code with $R = 1/2$ is used for upper branch encoding, where the generator in octal is $[5\ \ 7]$, with a minimum free distance of $d_{free} = 5$.

Modulation: OFDM vs. FDM. Under these settings, it then follows from Eq. (16) and Eq. (17) that the spectral efficiency for non-overlapping modulation is $\eta_{FDM} \approx 0.39$ bits/s/Hz, and $\eta_{OFDM} \approx 0.76$ bits/s/Hz for overlapping modulation. The overall bit error rate (BER) performance of the proposed system using these two modulation schemes are presented in Fig. 3. The jamming ratio ρ varies as we evaluate the system performances. It is demonstrated that the full-band jamming, i.e., $\rho = 1$, results in worst performance. The underlying argument is that with the employment of coding and interleaving, the jammer has to spread the noise over the whole bandwidth to achieve best jamming effects. We can also see from Fig. 3 that when overlapping modulation is employed, the system is more susceptible to jamming noise and the BER performance is much worse than the non-overlapping scheme.

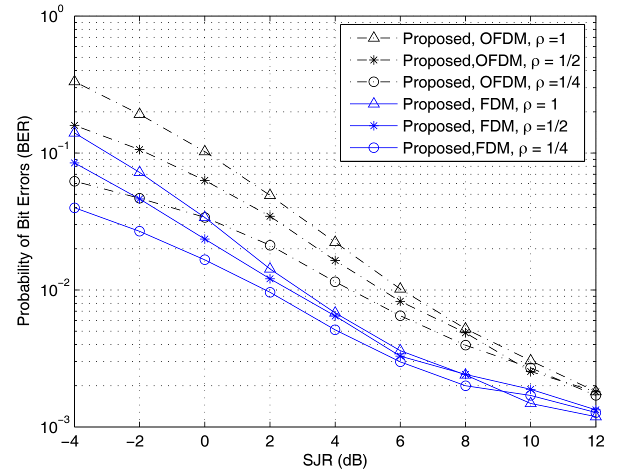

Fig. 3. BER performances of the proposed scheme, with non-overlapping and overlapping modulations, and varied jamming bandwidth.

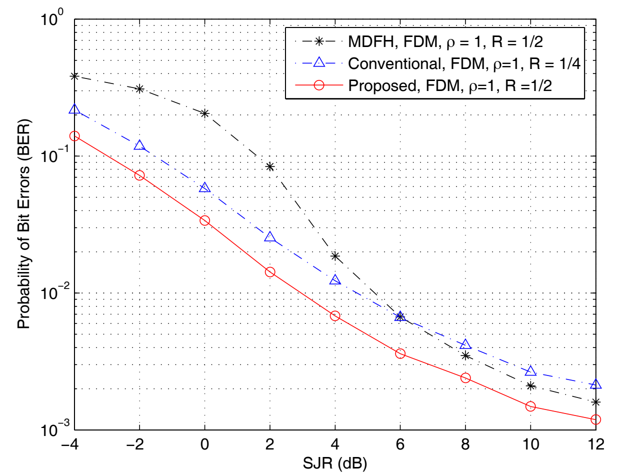

Fig. 4. Comparison of the proposed scheme (with R=1/2), the conventional unhopped scheme (with R=1/4), and the MDFH (with R=1/2), with $\rho = 1$.

Performance against conventional unhopped systems. Conventional unhopped schemes modulate all carriers with signals and possess poor jamming mitigation capabilities. In Fig. 4, we compare the BER performance of the proposed scheme and that of the conventional unhopped scheme. Both schemes use non-overlapping modulation (i.e., FDM). However, instead of using the half-rate convolutional code, the conventional unhopped scheme employs an $R = 1/4$ convolutional code such that its spectral efficiency (0.375 bits/s/Hz) is close to that of the proposed system (0.39 bits/s/Hz). The generator in octal is $[5\ \ 7\ \ 7\ \ 7]$ with a corresponding minimum free distance of $d_{free} = 10$. We can see that a 2dB gain can be achieved by the proposed scheme, which substantiates the effectiveness of the scheme's anti-jamming capability.

Performance against the MDFH scheme. Fig. 4 also presents the BER comparison of the proposed scheme and the MDFH. The same half-rate convolutional code and same

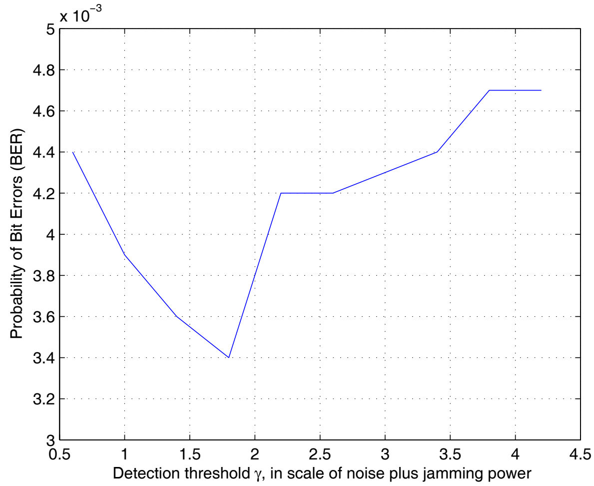

Fig. 5. Performance under different detection thresholds γ, which is represented in scale of noise plus jamming power, with $\rho = 1$ and $SJR = 6dB$.

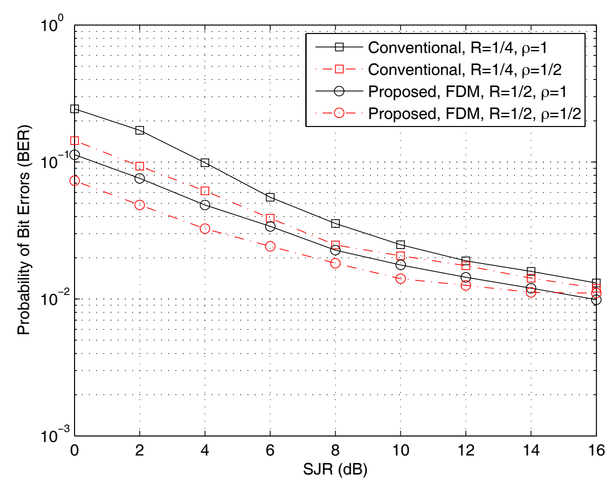

Fig. 6. Performance under fading channels: the proposed scheme (with R=1/2) and the conventional unhopped scheme (with R=1/4), with $\rho = 1$ and $\rho = 1/2$.

symbol mapping are employed for both schemes. According to the analysis in [8], when the MDFH divides $N = 128$ frequency bands into $N_g = 16$ groups, a spectral efficiency of 0.375 bits/s/Hz can be achieved, which is close to that of the proposed scheme. Under these settings, as shown in Fig. 4, the proposed scheme possesses better anti-jamming capabilities than the MDFH. The performance improvement is mainly caused by the effective hopping pattern retrieval mechanisms inherent in the proposed scheme.

Effect of threshold γ. The effect of detection threshold γ on system performance is demonstrated in Fig. 5, where the curve represents the BER of the proposed scheme under full-band jamming when the detection threshold γ varies. The horizontal axis is the value of γ in scale of noise plus jamming power. It can be seen that the BER performance is not very sensitive to the value of γ: the system achieves the optimal performance when γ is in the range of one to two times of noise plus jamming power, but satisfying performance still holds even if γ deviates from the optimal range. Analytical result on this can be found in [12].

Performance under fading channels. Fig. 6 illustrates the performances of the proposed system and the conventional unhopped system under fading channels. We consider Rayleigh distributed frequency selective fading caused by multipath propagation. Intuitively, the intersymbol interference caused by multipath fading can be regarded as self-jamming. Note that multicarrier communication is utilized, the fading is therefore flat over each channel. We assume that the channel state information can be estimated at the receiver. The received signals are equalized and then go through the signal extraction process. As shown in Fig. 6, where $SNR = 10dB$, fading does degrade the system performances as expected. However, under strong jamming interference, the proposed scheme still has performance gains over the unhopped system.

VI. Conclusions

In this paper, we propose a spectrally efficient anti-jamming system based on code controlled frequency hopping. Multiple frequency bands are randomly selected and modulated with message signals. Block coding is used for the receiver to correctly retrieve the frequency hopping patterns. The proposed scheme can effectively mitigate jamming interference, and meanwhile keep a high spectral efficiency. It provides a promising solution for efficient and secure wireless communications under jamming interferences.

References

[1] M. K. Simon, J. K. Omura, R. A. Scholtz, and B. K. Levitt, *Spread Spectrum Communications Handbook*, 2nd edition. McGraw-Hill, 2002.

[2] Y. Lam and P. Wittke, "Frequency-hopped spread-spectrum transmission with band-efficient modulations and simplified noncoherent sequence estimation," *IEEE Trans. Commun.*, vol. 38, 1990.

[3] K. C. Peng, C. H. Huang, C. J. Li, and T. S. Horng, "High-performance frequency-hopping transmitters using two-point delta-sigma modulation," *IEEE Trans. Microw. Theory Tech.*, vol. 52, 2004.

[4] S. Glisic, Z. Nikolic, N. Milosevic, and A. Pouttu, "Advanced frequency hopping modulation for spread spectrum WLAN," *IEEE J. Sel. Areas Commun.*, vol. 18, 2000.

[5] R. Ghareeb and A. Yongacoglu, "Performance analysis of frequency hopped/coherent MPSK in the presence of multitone jamming," *IEEE Trans. Commun.*, vol. 44, pp. 152-155, Feb. 1996.

[6] T. Scholand, T. Faber, A. Seebens, P. Jung, J. Lee, J. Cho, Y. Cho, and H. Lee, "Fast frequency hopping OFDM concept," *Electron. Lett.*, vol. 41, no. 13, pp. 748-749, 2005.

[7] Q. Ling, J. Ren, and T. Li, "Spectrally efficient spread spectrum system design: message-driven frequency hopping," in *Proc. IEEE International Conf. Commun. 2008*, pp. 4775-4779.

[8] Q. Ling and T. Li, "Message-driven frequency hopping-design and analysis," *IEEE Trans. Wireless Commun.*, vol. 8, no. 4, 2009, pp. 1773-1782.

[9] J. G. Proakis, *Digital Communications*, 4th edition. McGraw-Hill, 2000.

[10] M. Simon and A. Polydoros, "Coherent detection of frequency-hopped quadrature modulations in the presence of jamming–part I: QPSK and QASK modulations," *IEEE Trans. Commun.*, vol. 29, no. 11, pp. 1644-1660, 1981.

[11] C. Cook and H. Marsh, "An introduction to spread spectrum," *IEEE Commun. Mag.*, vol. 21, pp. 8-16, Mar. 1983.

[12] M. Schwartz, W. R. Bennett, and S. Stein, *Communication Systems and Techniques*. Wiley-IEEE Press, 1995.